STABILITY ANALYSIS OF A THIN MICROPOLAR FLUID FLOWING ON A ROTATING CIRCULAR DISK

C. K. Chen [*]

Department of Mechanical Engineering
National Cheng Kung University
Tainan, Taiwan 70101, R.O.C.

M. C. Lin [**]

Department of Mechanical Engineering
National Kaohsiung University of Applied Sciences
Kaohsiung, Taiwan 80778, R.O.C.

C. I. Chen [***]

Department of Industrial Engineering and Management
I-Shou University
Kaohsiung County, Taiwan 84041, R.O.C.

ABSTRACT

The stability analysis of a thin micropolar fluid flowing on a rotating circular disk is investigated numerically. The target is restricted to some neighborhood of critical value in the linear stability analysis. First, a generalized nonlinear kinematic model is derived by the long wave perturbation method. The method of normal mode is applied to the linear stability. After the weakly nonlinear dynamics of a film flow is studied by using the method of multiple scales, the Ginzburg-Landau equation is determined to discuss the necessary condition in terms of the various states of subcritical stability, subcritical instability, supercritical stability, and supercritical explosion for the existence of such flow pattern. The modeling results indicate that the rotation number and the radius of circular disk play the significant roles in destabilizing the flow. Furthermore, the micropolar parameter K serves as the stabilizing factor in the thin film flow.

Keywords : Nonlinear stability, Micropolar fluid, Ginzburg-Landau equation.

1. INTRODUCTION

A process for coating a surface on a spinning substrate, wherein a liquid coating material is dispensed radially from the center to the edge or from the edge to the center above the surface, and after application of the coating material the coating is cured. This process usually referred to as spin coating. To control the uniform and stable thin film is an interesting subject in the technological development for photolithography in wafer manufacturing [1-2]. Emslie *et al*. [3] was the pioneer who analyzed a Newtonian liquid flowing on a rotating disk. The flow is governed by a balance between the centrifugal force and the viscous resisting force. It was shown that the non-uniform distribution in the initial film profile tends to become uniform during spinning. This model has been widely employed in the subsequent investigations. Higgins [4] analyzed the flow of a Newtonian liquid placed on an impulsively started rotating disk. This work assumed a uniform film thickness and used the method of matched asymptotic expansions. It is showed that for films that maintain a planar interface there exists a self-similar form for the velocity field that allows the radial dependence to be factored out of the Navier-Stokes equations and boundary conditions. Kitamura *et al*. [5] solved the unsteady thin liquid film flow of non- uniform thickness on a rotating disk by asymptotic methods.

The linear stability theories for various film flows have been clearly presented by Lin [6] and Chandrasekhar [7]. Kapitza [8] was the first one to study the stability of a film flow over inclined planes. Various stability behaviors of the layer flows were analyzed. Benney [9] studied the non-linear evolution equation for free surfaces of the film flows by using the method of small parameters. The theory of Kapitza was later found not so compatible with the nonlinear theory of Landau [10]. The same film flow stability problem was studied by Yih [11] using a numerical approach. The transition mechanism from laminar flow to turbulent flow was elegantly explained by the Landau equation. This study shed a light later for further development on the theory of nonlinear film stability. The Landau equation was re-derived by Stuart [12] using the disturbed energy balance equation and Reynolds stresses. Pumir *et al*. [13] further included the effect of surface tension in the film flow model and solved for the solitary wave solutions. Ruyer-Quil and Manne-

[*] Professor, corresponding author [**] Postdoctoral Research Associate [***] Professor

DOI : 10.1017/jmech.2011.11

Copyright © 2011 The Society of Theoretical and Applied Mechanics, R.O.C.
https://doi.org/10.1017/jmech.2011.11 Published online by Cambridge University Press

ville [14-16] derived several models of the film flows down an inclined plane by the numerical simulation. The results indicate that it allows to better capture the viscous effects which are dominant at small Reynolds numbers. Amaouche *et al*. [17] showed an accurate modeling of a wavy film flow down an inclined plane in the inertia dominated regimes by using the weighted residual technique. It is shown the model follows quite closely, for a suitable choice of α, the Orr-Sommerfeld equation for all Weber and Kapitza numbers, in linear stability analysis. Samanta [18] derived the wave solution of a viscous film flowing down on a vertical non-uniformly heated wall. The results indicate that supercritical unstable region increases and the subcritical stable region decreases with the increase of Peclet number.

The theory of micropolar fluids has received much attention and this is because the traditional Newtonian fluids cannot precisely describe the characteristics of the fluid flow with suspended particles. Micropolar fluid theory was introduced by Eringen [19] in which coupling between the spin of each particle and the macroscopic velocity field is taken into account. The micropolar fluids may be used to model some manmade fluids, such as the polymeric fluids and liquid crystals, *etc*. Due to various applications, attention is gradually focused on this subject. Hung *et al*. [20] employed the method of nonlinear analysis to study the stability of thin micropolar liquid films flowing down a vertical plate. The results of their study indicated that the micropolar parameter K ($=\kappa/\mu$) plays an important role in stabilizing the film flow. Dupuy *et al*. [21] studied the flow of a micropolar fluid through a wavy constricted channel which depends on a small parameter by the asymptotic analysis. The results indicate that this method reduces the initial problem to the problem set in the boundary layers domain. Chen [22] studied the nonlinear stability characterization of the thin micropolar liquid film flowing down the inner surface of a rotating vertical cylinder. The results indicated that by increasing the rotation speed, and the radius of cylinder, the film flow will generally stabilize the flow system.

In this paper the authors are interested in investigating the existence of the supercritical and subcritical regions for a thin micropolar fluid flowing on a rotating circular disk. It is assumed that the disk radius is much larger than film thickness. Therefore, the peripheral effect is neglected by comparing with total film area [5]. The influence of the rotating motion, the disk size and micropolar effect on the equilibrium finite amplitude is studied and characterized mathematically. In an attempt to verify computational results and to illustrate the effectiveness of the proposed modeling approach, several numerical examples are also presented.

2. GENERALIZED KINEMATIC EQUATION

Figure 1 shows the appropriate physical configuration of a thin micropolar fluid flowing on a rotating

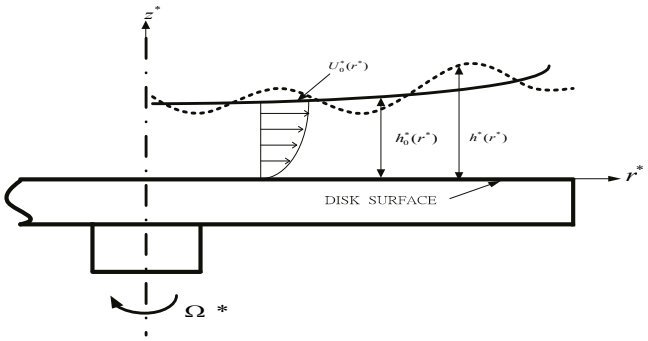


Fig. 1 Schematic diagram of a thin micropolar fluid flowing on a rotating circular disk

circular disk. In this case, all associated physical properties and rate of film flow are assumed to be constant (*i.e.* time-invariant). The centripetal acceleration is the only driving force considered. The principles of mass and momentum conservation for an axis-symmetric isothermal incompressible film flow lead to a set of governing equations. Let u^* and w^* be the velocity components in the radial direction r^* and the perpendicular direction z^* of the disk. The variable with a superscript " * " stands for a dimensional quantity. The governing equations can be expressed in terms of cylindrical coordinates (r^*, z^*) as [19]

$$\frac{1}{r^*}\frac{\partial(r^*u^*)}{\partial r^*}+\frac{\partial w^*}{\partial z^*}=0 \tag{1}$$

$$\rho\left(\frac{\partial u^*}{\partial t^*}+u^*\frac{\partial u^*}{\partial r^*}+w^*\frac{\partial w^*}{\partial z^*}-\frac{v^{*2}}{r^*}\right)=$$
$$-\frac{\partial p^*}{\partial r^*}+(\mu+k)\left(\frac{\partial^2 u^*}{\partial r^{*2}}+\frac{1}{r^*}\frac{\partial u^*}{\partial r^*}+\frac{\partial^2 u^*}{\partial z^{*2}}-\frac{u^*}{r^{*2}}\right)-k\frac{\partial N^*}{\partial z^*} \tag{2}$$

$$\rho\left(\frac{\partial w^*}{\partial t^*}+u^*\frac{\partial w^*}{\partial r^*}+w^*\frac{\partial w^*}{\partial z^*}\right)=$$
$$-\frac{\partial p^*}{\partial z^*}-\rho g+(\mu+k)\left(\frac{\partial^2 w^*}{\partial r^{*2}}+\frac{1}{r^*}\frac{\partial w^*}{\partial r^*}+\frac{\partial^2 w^*}{\partial z^{*2}}\right)+k\left(\frac{\partial N^*}{\partial r^*}+\frac{N^*}{r^*}\right) \tag{3}$$

$$\rho J\left(\frac{\partial N^*}{\partial t^*}+u^*\frac{\partial N^*}{\partial r^*}+w^*\frac{\partial N^*}{\partial z^*}\right)=$$
$$\gamma\left(\frac{\partial^2 N^*}{\partial r^{*2}}+\frac{1}{r^*}\frac{\partial N^*}{\partial r^*}+\frac{\partial^2 N^*}{\partial z^{*2}}-\frac{N^*}{r^{*2}}\right)+k\left(\frac{\partial u^*}{\partial z^*}-\frac{\partial w^*}{\partial r^*}-2N^*\right) \tag{4}$$

where v^* is the tangential velocity, ρ is the density of the fluid, p^* is the fluid pressure, g is the gravitational acceleration, μ is the fluid dynamic viscosity, k is the vortex viscosity, N^* is the angular micro-rotation momentum, J is the micro-inertial density and γ is the spin-gradient viscosity. On the disk surface $z^*=0$. The boundary conditions are treated as non-slip as

$$u^*=0 \tag{5}$$

https://doi.org/10.1017/jmech.2011.11 Published online by Cambridge University Press

$$w^* = 0 \tag{6}$$

$$N^* = \frac{1}{2}\left(\frac{\partial u^*}{\partial z^*}\right) \tag{7}$$

On the free surface $z^* = h^*$, The boundary condition approximated by the vanishing of shear stress is expressed as

$$\left(\frac{\partial u^*}{\partial z^*} + \frac{\partial w^*}{\partial r^*}\right)\left(1 - \left(\frac{\partial h^*}{\partial r^*}\right)^2\right) - 2^*\left(\frac{\partial u^*}{\partial r^*} - \frac{\partial w^*}{\partial z^*}\right)\left(\frac{\partial h^*}{\partial r^*}\right) = 0 \tag{8}$$

The normal stress condition obtained by solving the balance equation in the direction normal to the free surface is given as

$$p^* + 2\mu\left(1 + \left(\frac{\partial h^*}{\partial r^*}\right)^2\right)^{-1}\left[\frac{\partial h^*}{\partial r^*}\left(\frac{\partial u^*}{\partial z^*} + \frac{\partial w^*}{\partial r^*}\right) - \frac{\partial w^*}{\partial z^*} - \frac{\partial u^*}{\partial r^*}\left(\frac{\partial h^*}{\partial r^*}\right)^2\right] + S^*\frac{\partial^2 h^*}{\partial r^{*2}}\left[1 + \left(\frac{\partial h^*}{\partial r^*}\right)^2\right]^{-3/2} = p_a^* \tag{9}$$

$$\frac{\partial u^*}{\partial z^*} = N^* = 0 \tag{10}$$

where h^* is the local film thickness, S^* is surface tension and p_a^* is the atmosphere pressure. The boundary conditions given in Eqs. (7) and (10) for N^* at solid wall and at free surface are shown in Ahmadi [23] and Jena and Mathur [24].

The kinematic condition that the flow does not travel across a free surface can be given as

$$\frac{\partial h^*}{\partial t^*} + \frac{\partial h^*}{\partial r^*}u^* - w^* = 0 \tag{11}$$

By introducing a stream function φ^*, the dimensional velocity components can be expressed as

$$u^* = \frac{1}{r^*}\frac{\partial \varphi^*}{\partial z^*},\ w^* = -\frac{1}{r^*}\frac{\partial \varphi^*}{\partial r^*} \tag{12}$$

The following variables are used to form the dimensionless governing equations and boundary conditions

$$z = \frac{z^*}{h_0^*},\ r = \frac{\alpha r^*}{h_0^*},\ t = \frac{\alpha t^* u_0^*}{h_0^*},\ h = \frac{h^*}{h_0^*},\ \varphi = \frac{\alpha\varphi^*}{u_0^* h_0^{*2}},$$
$$p = \frac{p^* - p_a^*}{\rho u_0^{*2}},\ N = \frac{N^* h_0^*}{u_0^*},\ \mathrm{Re} = \frac{u_0^* h_0^*}{\nu},\ \Lambda = \frac{\gamma}{\mu J},$$
$$K = \frac{k}{\mu},\ \Delta = \frac{h_0^{*2}}{J},\ Fr = \frac{g h_0^*}{u_0^{*2}},\ S = \frac{S^*}{\rho u_0^{*2} h_0^*},\ \alpha = \frac{2\pi h_0^*}{\lambda}, \tag{13}$$

where h_0^*, α, u_0^*, Re, ν, Fr, λ are the average film thickness, perturbed wavelength, scale of velocity, Reynolds number, the kinematic viscosity, Froude number, dimensionless wavenumber, respectively. Furthermore, the Λ and the Δ are the micropolar parameters. For simplification, it is assumed that the fluid film is very thin ($h^* << r^*$). In consequence, it is reasonable to assume that the tangential velocity is constant throughout the radial direction in the thin film, *i.e.* $v^* = r^*\Omega^*$. In order to investigate the effect of angular velocity, Ω^*, on the stability of the flow field, the dimensionless parameter *Ro* (rotation number) is defined as

$$Ro = \frac{\Omega^* h_0^*}{u_0^*} \tag{14}$$

In terms of these non-dimensional variables, the equations of motion become

$$(1+K)r^{-1}\varphi_{zzz} = -\mathrm{Re}\, rRo^2 + \alpha\,\mathrm{Re}\left[p_r + (1+K)(r^{-1}\varphi_{tz} + r^{-2}\varphi_z\varphi_{rz} - r^{-3}\varphi_z^2 - r^{-2}\varphi_r\varphi_{zz}) - KN_Z\right] + O(\alpha^2) \tag{15}$$

$$p_z = -Fr + \alpha\left((1+K)(-\mathrm{Re}^{-1}r^{-1}\varphi_{rzz}) + Kr^{-1}(rN)_r\right) + O(\alpha^2) \tag{16}$$

$$\Lambda N_{zz} - 2K\Delta N + K\Delta(r^{-1}\varphi_r)_r = \alpha\,\mathrm{Re}(N_t + r^{-1}\varphi_z N_r - r^{-1}\varphi_r N_z) + O(\alpha^2) \tag{17}$$

Using the non-dimensional variables, the boundary conditions at the surface of disk $z = 0$ reduces to

$$\varphi = \varphi_z = 0 \tag{18}$$

$$N = 2^{-1}(r^{-1}\varphi_z)_z + O(\alpha^2) \tag{19}$$

And the boundary conditions at the free surface of disk $z = h$ becomes

$$r^{-1}\varphi_{zz} = \alpha^2\left[r^{-1}\varphi_{rr} - r^{-2}\varphi_r + 2h_r(1-\alpha^2 h_r^2)^{-1}(2r^{-1}\varphi_{rz} - r^{-2}\varphi_z)\right] \tag{20}$$

$$p = -S\alpha^2 h_{rr}(1+\alpha^2 h_r^2)^{-3/2} + \alpha\left[-2\,\mathrm{Re}^{-1}(1+\alpha^2 h_r^2)^{-1}(r^{-1}\varphi_{rz} + r^{-1}\varphi_{zz} h_r)\right] + O(\alpha^2) \tag{21}$$

$$N = 0 \tag{22}$$

$$h_t + r^{-1}h_r\varphi_z + r^{-1}\varphi_r = 0 \tag{23}$$

Hence the term $\alpha^2 S$ can be treated as a quantity of zeroth order [20]. Since the modes of long-wavelength that gives the smallest wave number are most likely to induce flow instability for the film flow, this can be done by expanding the stream function, flow pressure and the angular micro-rotation momentum in terms of some small wave number ($\alpha << 1$) as

https://doi.org/10.1017/jmech.2011.11 Published online by Cambridge University Press

$$\varphi = \varphi_0 + \alpha\varphi_1 + O(\alpha^2) \tag{24}$$

$$p = p_0 + \alpha p_1 + O(\alpha^2) \tag{25}$$

$$N = N_0 + \alpha N_1 + O(\alpha^2) \tag{26}$$

The flow conditions of the thin film can be obtained by inserting above expressions into Eqs. (15) ~ (23) and then solving systematically the resulting equations. Furthermore, Hung *et al*. [20] showed that the micropolar parameter Λ has very little effect on the stability of the micropolar film. For simplifying the solved equations that gives no spin-gradient viscosity effect, neglecting the Λ term in Eq. (17), by collecting all terms of zeroth-order (α°) in the governing equations, the set of zeroth- order equations can now be expressed as

$$(1+K)\, r^{-1}\varphi_{0zzz} = -\mathrm{Re}\, r\, Ro^2 \tag{27}$$

$$p_{0z} = -Fr + Kr^{-1}(rN_0)_r \tag{28}$$

$$-2K\Delta N_0 + K\Delta(r^{-1}\varphi_{0r})_r = 0 \tag{29}$$

The boundary conditions associated with the equations of zeroth-order are given as

$$z = 0$$

$$\varphi_0 = \varphi_{0z} = 0 \tag{30}$$

$$N_0 = 2^{-1}(r^{-1}\varphi_{0z})_z \tag{31}$$

$$z = h$$

$$r^{-1}\varphi_{0zz} = 0 \tag{32}$$

$$p_0 = -S\alpha^2 h_{rr} \tag{33}$$

$$N_0 = 0 \tag{34}$$

After collecting all terms of first-order (α^1) in the governing equations, the first-order equations can be rearranged as

$$(1+K)r^{-1}\varphi_{1zzz} = \mathrm{Re}\Big[\, p_{0r} + (1+K)(r^{-1}\varphi_{0tz} + r^{-2}\varphi_{0z}\,\varphi_{0rz} - r^{-3}\varphi_{0z}^2 - r^{-2}\varphi_{0r}\,\varphi_{0zz}) - KN_{0z}\Big] \tag{35}$$

$$p_{1z} = -(1+K)\,\mathrm{Re}^{-1}\, r^{-1}\varphi_{0rzz} + Kr^{-1}(rN_0)_r \tag{36}$$

$$-2K\Delta N_1 + K\Delta(r^{-1}\varphi_{1r})_r = \mathrm{Re}(N_{0t} + r^{-1}\varphi_{0z}\, N_{0r} - r^{-1}\varphi_{0r}\, N_{0z})\,. \tag{37}$$

The corresponding boundary conditions are given as

$$z = 0$$

$$\varphi_1 = \varphi_{1z} = 0 \tag{38}$$

$$N_1 = 2^{-1}(r^{-1}\varphi_{1z})_z \tag{39}$$

$$z = h$$

$$r^{-1}\varphi_{1zz} = 0 \tag{40}$$

$$p_1 = -2\,\mathrm{Re}^{-1}(r^{-1}\varphi_{0rz} + r^{-1}\varphi_{0zz}\, h_r) \tag{41}$$

$$N_1 = 0 \tag{42}$$

The solutions of the zeroth-order and first-order equations are given in Appendix *A*.

By substituting the zeroth-order and the first-order solutions into the dimensionless free surface kinematic equation of Eq. (23), the generalized nonlinear kinematic equation is obtained and presented as

$$h_t + A(h)h_r + B(h)h_{rr} + C(h)h_{rrr} + D(h)h_{rrrr} + E(h)h_r^2 + F(h)h_r\, h_{rrr} = 0 \tag{43}$$

Where $A(h)$, $B(h)$, $C(h)$, $D(h)$, $E(h)$ and $F(h)$ are given in Appendix *B*.

3. STABILITY ANALYSIS

When the variation of film thickness is small in the base flow, it is assumed to assign the local dimensionless film thickness a value of one. For small amplitude-regimes, we have $\eta(r, t) << 1$, the dimensionless film thickness when expressed in perturbed state can be given as

$$h(r,\, t) = 1 + \eta(r,\, t) \tag{44}$$

where η is a perturbed quantity to the stationary film thickness. Substituting the value of $h(r, t)$ into the evolution Eq. (43) and all terms up to the order of η^3 are collected, the evolution equation of η can be obtained and given as

$$\begin{aligned}\eta_t + A\eta_r + B\eta_{rr} + C\eta_{rrr} + D\eta_{rrrr} + E\eta_r^2 + F\eta_r\,\eta_{rrr} \\ = \Big[\Big(A'\eta + \frac{A''}{2}\eta^2\Big)\,\eta_r + \Big(B'\eta + \frac{B''}{2}\eta^2\Big)\,\eta_{rr} \\ + \Big(C'\eta + \frac{C''}{2}\eta^2\Big)\,\eta_{rrr} + \Big(D'\eta + \frac{D''}{2}\eta^2\Big)\,\eta_{rrrr} \\ + (E + E'\eta)\,\eta_r^2 + (F + F'\eta)\,\eta_r\eta_{rrr}\Big] + O(\eta^4)\end{aligned} \tag{45}$$

where the values of *A, B, C, D, E, F* and their derivatives are all evaluated at the dimensionless height of the film $h(r, t) = 1$.

3.1 Linear Stability Analysis

As the nonlinear terms of Eq. (45) are neglected, the linearized equation is given as

$$\eta_t + A\eta_r + B\eta_{rr} + C\eta_{rrr} + D\eta_{rrrr} = 0 \tag{46}$$

In order to use the normal mode analysis, we assume that

$$\eta = a\exp\big[i(r - dt)\big] + c.c. \tag{47}$$

https://doi.org/10.1017/jmech.2011.11 Published online by Cambridge University Press

where a is the perturbation amplitude, c.c. is the complex conjugate counterpart, and r, t are the fast scales. The complex wave celerity, d is given as

$$d = d_r + id_i = (A - C) + i(B - D) \tag{48}$$

where d_r and d_i are regarded as the linear wave speed and linear growth rate of the disturbance, respectively. The solution of the disturbance about $h(r, t) = 1$ is asymptotically stable or unstable according as $d_i < 0$ or $d_i > 0$. This is equivalent to the inequality of $B < D$ or $B > D$.

3.2 Weakly Nonlinear Stability Analysis

Nonlinear effects, when they are weak enough, do not fundamentally alter the nature of the motion. A weakly nonlinear solution can be usefully expressed as weak stability or instability, but the definition is restricted to some neighborhood of critical value. In this paper the authors are interested in investigating the existence of the supercritical and subcritical regions. In order to characterize the weakly nonlinear behaviors of thin film flows, the method of multiple scales [6] is employed here and the resulting Ginburg-Landau equation [24] can be derived following the same procedure as Chen *et al.* [22] and Cheng and Lai [26]

$$\frac{\partial a}{\partial t_2} + D_1 \frac{\partial^2 a}{\partial r_1^2} - \varepsilon^{-2} d_i\, a + (E_1 + iF_1)\, a^2\, \bar{a} = 0 \tag{49}$$

Where ε is a small perturbation parameter, and the slow scales $t_2 = \varepsilon^2 t$, $r_1 = \varepsilon r$. Here $\bar{a}$ stands for the complex conjugate of perturbation amplitude, and

$$e = e_r + ie_i = \frac{(B' - D' + E - F)(16D - 4B) + 6C(A' - C')}{(16D - 4B)^2 + 36C^2} + i\frac{6C(B' - D' + E - F) - (A' - C')(16D - 4B)}{(16D - 4B)^2 + 36C^2} \tag{50}$$

$$D_1 = \left[(B - 6D) + i(3C)\right] \tag{51}$$

$$E_1 = (-5B' + 17D' + 4E - 10F)\, e_r - (A' - 7C')\, e_i + \left(-\frac{3}{2}B'' + \frac{3}{2}D'' + E' - F'\right) \tag{52}$$

$$F_1 = (-5B' + 17D' + 4E - 10F)\, e_i + (A' - 7C')\, e_r + \frac{1}{2}(A'' - C'') \tag{53}$$

Equation (49) can be used to investigate the weak nonlinear behavior of the film flow. In order to solve for Eq. (49), we assume a filtered wave with no spatial modulation. So for a filtered wave a can be given as

$$a = a_0 \exp\left[-ib(t_2)\, t_2\right] \tag{54}$$

A fter substituting Eqs. (54) into (49), one can obtain

$$\frac{\partial a_0}{\partial t_2} = (\varepsilon^{-2} d_i - E_1\, a_0^2)\, a_0 \tag{55}$$

$$\frac{\partial \left[b(t_2)\, t_2\right]}{\partial t_2} = F_1\, a_0^2 \tag{56}$$

The threshold amplitude εa_0 in the supercritical stable region is given as

$$\varepsilon a_0 = \sqrt{\frac{d_i}{E_1}} \tag{57}$$

The nonlinear wave speed Nc_r is given as

$$Nc_r = d_r + d_i\left(\frac{F_1}{E_1}\right) \tag{58}$$

If $E_1 = 0$, the Eq. (55) is reduced to a linear equation. The second term on the right-hand side of Eq. (55) is due to the nonlinearity and may moderate or accelerate the exponential growth of the linear disturbance according to the signs of d_i and E_1. Equation (56) is used to modify the perturbed wave speed caused by infinitesimal disturbances appearing in the nonlinear system. The condition for the film flow to present the behavior of subcritical instability in the linearly stable region ($d_i < 0$) is given as $E_1 < 0$, and the threshold amplitude of the wave is given as εa_0. The subcritical stable region can only be found as $E_1 > 0$. The neutral stability curve can only be derived and plotted for the condition of $E_1 = 0$. The Ginzburg–Landau equation can be used to characterize various flow states, with the results summarized in Table 1.

Table 1 Various states of Landau equation

Linearly stable (subcritical region) $d_i < 0$	subcritical instability $E_1 < 0$	$\varepsilon a_0 < (d_i / E_1)^{1/2}$	$a_0 \to 0$	Conditional Stability
		$\varepsilon a_0 > (d_i / E_1)^{1/2}$	$a_0 \uparrow$	Subcritical explosive State
	subcritical (absolute) stability $E_1 > 0$	$A_0 \to 0$		
Linearly unstable (supercritical region) $d_i > 0$	supercritical explosive state $E_1 < 0$	$a_0 \uparrow$		
	supercritical stability $E_1 > 0$	$\varepsilon a_0 < (d_i / E_1)^{1/2}$ $Nc_r \to d_r + d_i (F_1 / E_1)$		

https://doi.org/10.1017/jmech.2011.11 Published online by Cambridge University Press

4. NUMERICAL ILLUSTRATION AND DISCUSSIONS

Based on modeling results, the condition for the stability behaviors of a thin film flow can be expressed as a function of Reynolds number, Re, rotation number, Ro, dimensionless perturbation wave number, α, dimensionless radius of circular disk, r and micropolar parameter, K, respectively. In order to study the effects of dimensionless radius, rotation number and micropolar parameter on the stability of a thin flow, we select randomly but within specified ranges physical parameters for numerical experiment. Physical parameters that are selected for study include (1) Reynolds numbers ranging from 0 to15, (2) The dimensionless perturbation wave numbers ranging from 0 to 0.12, (3) Rotation number including 0.1, 0.12 and 0.15, (4) The values of dimensionless radius including 50, 75 and 100, (5) The values of micropolar parameter K being 20, 22 and 25, (6) The value of micropolar parameter Δ being 10. The ranges for these above parameters are based on published reasonable ranges for these parameters [22]. Other of our parameters are treated as constants for all numerical computations since we are considering practical spin coating systems in which these variables are not expected to undergo significant variation. In practice, the parameter S is a large value. Further, for simplification analysis, α^2S, Re and Fr are taken to be of the same order (**O** (1)) [20,22], so the values of some dimensionless parameters are taken as, a constant dimensionless surface tension S = 6173.5 and Fr = 9.8.

4.1 Linear Stability Analysis

By setting $d_i = 0$ in the linear stability analysis, the neutral stability curve can be easily determined from Eq. (48). The α-Re plane is divided into two different characteristic regions by the neutral stability curve. One is the linearly stable region where small disturbances decay with time and the other is the linearly unstable region where small perturbations grow as time increases. Figure 2(a) shows that the stable region decreases and unstable region increases with an increase of rotation number. Figure 2(b) shows that the stable region decreases and unstable region increases with increasing radius of the circular disk. The reason for this phenomenon is the existence of the centrifugal force term, which is a radius-related force in the governing equation. To increase the radius and the rotation number results in accelerated growth of the linear disturbance due to the centrifugal force. Figure 2(c) shows that the stable region increases and unstable region decreases with an increase of the micropolar parameter K. Hence one can say that in linear stability analysis, the rotation number and the radius of circular disk give the same destabilizing effects, but the micropolar parameter K gives a stabilizing effect.

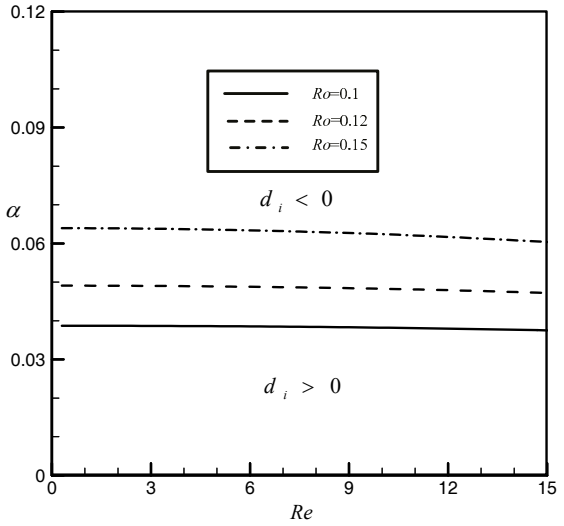


Fig. 2(a) Linear neutral stability curves for three different Ro values at r = 50 and K = 20

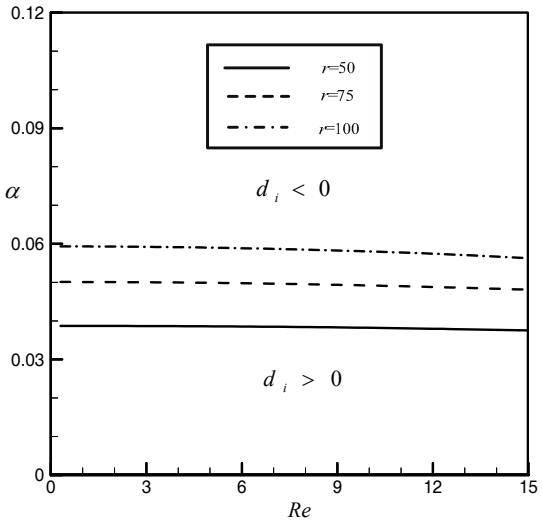


Fig. 2(b) Linear neutral stability curves for three different r values at K = 20 and Ro = 0.1

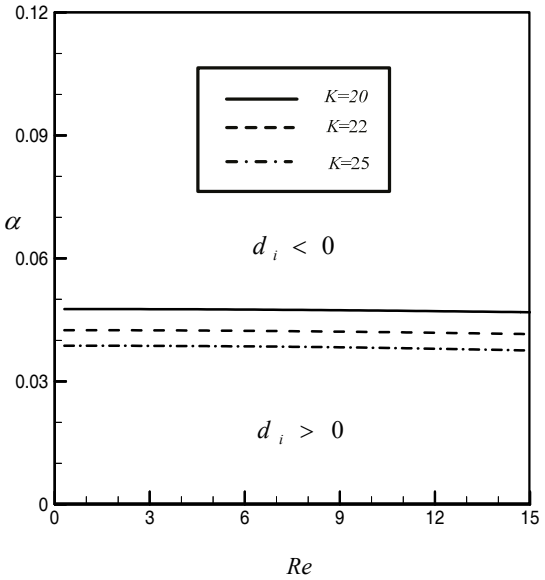


Fig. 2(c) Linear neutral stability curves for three different K values at r = 50 and Ro = 0.1

https://doi.org/10.1017/jmech.2011.11 Published online by Cambridge University Press

4.2 Weakly Nonlinear Stability Analysis

The main purpose of the nonlinear stability analysis is to study the weakly nonlinear analysis of the evolution equation. Figures 3(a) to 3(d) reveal that various conditions for the subcritical instability ($d_i < 0$, $E_1 < 0$), the subcritical stability ($d_i < 0$, $E_1 > 0$), the supercritical stability ($d_i > 0$, $E_1 > 0$) and the explosive supercritical instability ($d_i > 0$, $E_1 < 0$). Figure 4(a) shows the threshold amplitude in subcritical unstable region for various wave numbers with different Ro values at Re = 6, r = 50 and K = 20. The results indicate that the threshold amplitude εa_0 becomes smaller as the value of rotation number, Ro increases. Figure 4(b) shows the threshold amplitude in subcritical unstable region for various wave numbers with different values of radius, r at Re = 6, Ro = 0.1 and K = 20. The results indicate that the threshold amplitude εa_0 becomes smaller as the value of radius r changes from 50, 75, and 100. The reason for this phenomenon is the existence of the centrifugal force term, which is a radius-related force in the governing equation. As the size of radius and rotation number gradually increased, it may accelerate the growth of the linear disturbance due to the centrifugal force. In such situations, the film flow which holds the higher threshold amplitude value will become more stable than those that hold smaller one. If the initial finite-amplitude disturbance is less than the threshold amplitude, the system will become conditionally stable.

Figure 5(a) shows the threshold amplitude in the supercritical stability region for various wave numbers with different Ro values at Re = 12, r = 50 and K = 20. It is found that the decrease of rotation number will lower the threshold amplitude, and the flow will become relatively more stable. Figure 5(b) shows the threshold amplitude in the supercritical stability region for various wave numbers with different micropolar parameter values at Re = 12, r = 50 and Ro = 0.1. It is found that the increase of micropolar parameter will lower the threshold amplitude. The reason is that the part of the momentum is lost in rotating of the particles, so the vortex viscosity will lead to energy transfers between different waves and decay the amplitude of surface waves. The flow will become relatively more stable as the micropolar parameter increases.

The wave speed of Eq. (48) predicted by using the linear theory is a constant value for all wave number and rotation number. However, the wave speed of Eq. (58) predicted by using nonlinear theory is no longer a constant. It is actually a function of wave number, Reynolds number, rotation number, the radius of disk and micropolar parameter. Figure 6(a) shows the nonlinear wave speed in the supercritical region for various perturbed wave numbers and different Ro values at Re = 12, r = 50 and K = 20. Figure 6(b) shows the nonlinear wave speed in the supercritical stable region for various perturbed wave numbers and different micropolar parameter values at Re = 12, r = 50 and Ro = 0.1. It is found that the nonlinear wave speed increases as the value of rotation number increases or the micropolar parameter decreases.

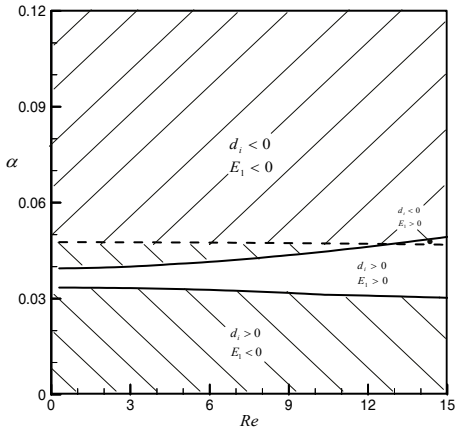


Fig. 3(a) Neutral stability curves of micropolar film flows for Ro = 0.1, r = 50 and K = 20

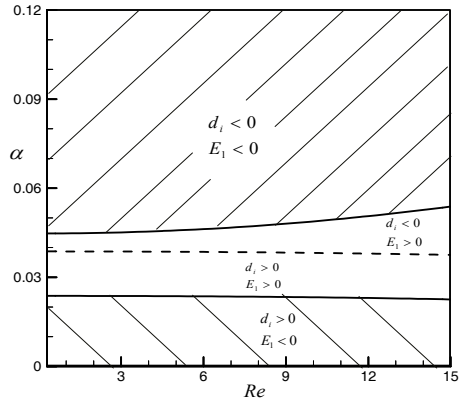


Fig. 3(b) Neutral stability curves of micropolar film flows for Ro = 0.1, r = 50 and K = 25

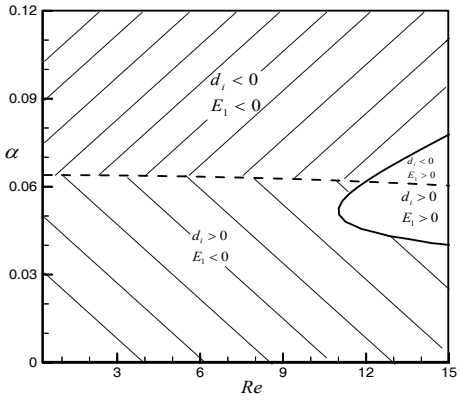


Fig. 3(c) Neutral stability curves of micropolar film flows for Ro = 0.15, r = 50 and K = 20

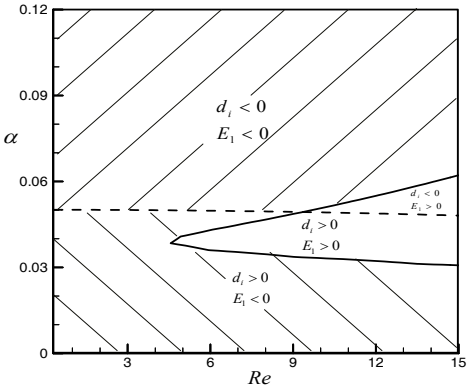


Fig. 3(d) Neutral stability curves of micropolar film flows for Ro = 0.1, r = 75 and K = 20

https://doi.org/10.1017/jmech.2011.11 Published online by Cambridge University Press

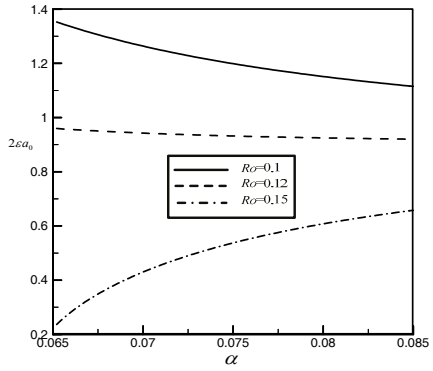


Fig. 4(a) Threshold amplitude in subcritical instability region for three different *Ro* values at Re = 6, $r = 50$ and $K = 20$

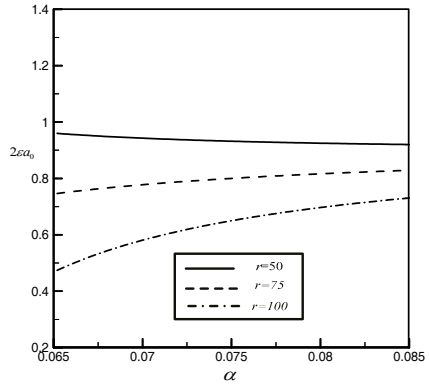


Fig. 4(b) Threshold amplitude in subcritical instability region for three different *r* values at Re = 6, $Ro = 0.1$ and $K = 20$

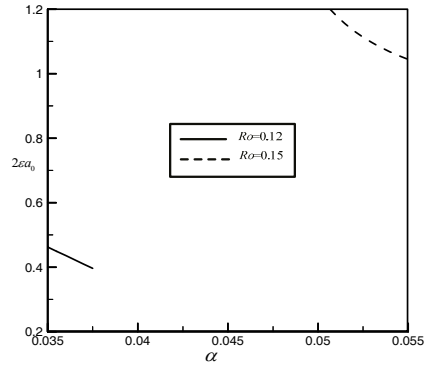


Fig. 5(a) Threshold amplitude in supercritical stability region for two different *Ro* values at Re = 12, $r = 50$ and $K = 20$

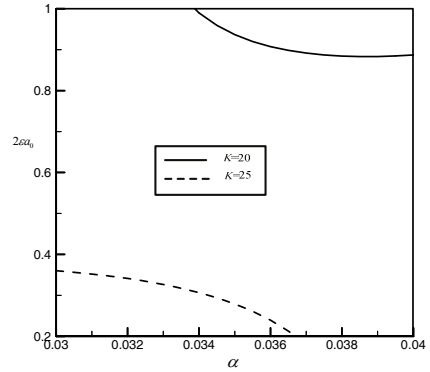


Fig. 5(b) Threshold amplitude in supercritical stability region for two different *K* values at Re = 12, $r = 50$ and $Ro = 0.1$

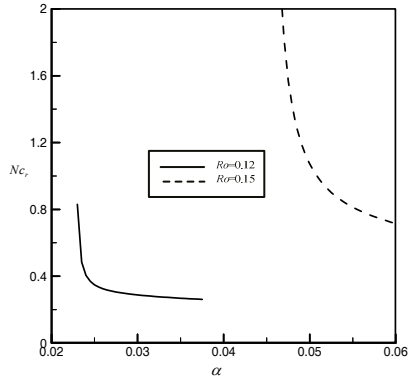


Fig. 6(a) Nonlinear wave speed in supercritical stability region for two different *Ro* values Re = 12, $r = 50$ and $K = 20$

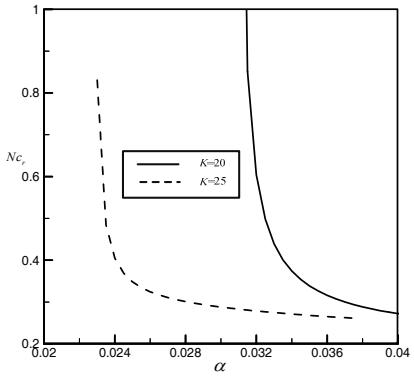


Fig. 6(b) Nonlinear wave speed in supercritical stability region for two different *K* values Re = 12, $r = 50$ and $Ro = 0.1$

5. CONCLUDING REMARKS

The stability analysis of a thin micropolar fluid flowing on a rotating circular disk is thoroughly investigated by using the method of long-wave perturbation. On the basis of the results of numerical modeling, several conclusions can be drawn as follows.

1. The modeling results indicate that the area of linearly stable region becomes smaller for an increasing rotation number or an increasing size of radius. Hence one can say that in linear stability analysis, the rotation number and the radius of circular disk give the same destabilizing effects.
2. The micropolar parameter *K* serves as the stabilizing factor in the thin film flow.
3. Weakly nonlinear stability analysis has successfully revealed the subcritical stability, subcritical instability, supercritical stability and supercritical explosion regions for the flow patterns of a thin film on a rotating disk. It is found that in subcritical instability region, the threshold amplitude εa_0 becomes smaller as the value of the rotation number or the radius of circular disk become larger. When the initial finite- amplitude disturbance is less than the threshold amplitude, the flow will be conditionally stable.

https://doi.org/10.1017/jmech.2011.11 Published online by Cambridge University Press

4. The increase of micropolar parameter K will lower the threshold amplitude in the supercritical stability region. The flow will become relatively more stable.

ACKNOWLEDGEMENTS

The authors sincerely thank the reviewers for their very useful comments and suggestions which have helped in improving the quality of this manuscript.

APPENDIX A

The solutions for the equations of zeroth-order can be given as

$$\varphi_0 = \frac{1}{6(1+K)}\, r^2\, \mathrm{Re}\, Ro^2 (3h - z)\, z^2$$

$$p_0 = Fr(h - z) - S\alpha^2 h_{rr}$$

$$N_0 = \frac{1}{4(1+K)}\, r^2\, \mathrm{Re}\, Ro^2 z^2 (3h_r + r h_{rr})$$

First-order solution can be given as

$$\varphi_1 = k_1 z^8 + k_2 z^7 + k_3 z^6 + k_4 z^5 + k_5 z^4 + k_6 z^3 + k_7 z^2 + k_8 z + k_9$$

$$N_1 = C_1 z^7 + C_2 z^6 + C_3 z^5 + C_4 z^4 + C_5 z^3 + C_6 z^2 + C_7 z + C_8$$

where

$$k_1 = -\frac{r^2 \cdot \mathrm{Re}^3 \cdot Ro^4}{2016(1+K)^2}$$

$$k_2 = \frac{\left(3 + K + 5h(1+k)\right)\, r^2 \cdot \mathrm{Re}^3 \cdot Ro^4}{1260(1+K)^3}$$

$$k_3 = -\frac{h\left(5 + 2K + 3h(1+k)\right)\, r^2 \cdot \mathrm{Re}^3 \cdot Ro^4}{360(1+K)^3}$$

$$k_4 = -\frac{h \cdot r^2 \cdot \mathrm{Re}^3 \cdot Ro^4 \left(2h(1+K) + (K-1)\, r \cdot h_r\right)}{120(1+K)^3}$$

$$k_5 = -\frac{K \cdot r \cdot \mathrm{Re} \cdot Ro^2 (3h_r + r \cdot h_{rr})}{48(1+K)}$$

$$k_6 = \frac{r \cdot \mathrm{Re}(Fr \cdot h_r - S \cdot \alpha^2 \cdot h_{rrr})}{6(1+K)}$$

$$k_7 = \frac{1}{360(1+K)^3}\Big(h \cdot r \cdot \mathrm{Re}\Big(h^4\left(-3 - 36K + 20h(1+K)\right)\, r \cdot \mathrm{Re}^2 \cdot Ro^4 - 15\Big(12Fr(1+K)^2 - 9h \cdot K(1+K)^2 Ro^2 + 2h^3(K-1)\, r^2 \cdot \mathrm{Re}^2 \cdot Ro^4\Big)\, h_r + 45h \cdot K(1+K)^2 r \cdot Ro^2 \cdot h_{rr} + 180(1+K)^2 S \cdot \alpha^2 \cdot h_{rrr}\Big)\Big)$$

$$k_8 = k_9 = 0$$

$$C_1 = \frac{\mathrm{Re}^3 \cdot Ro^4 (3h_r + r \cdot h_{rr})}{504(1+K)^2}$$

$$C_2 = -\frac{1}{720(1+K)^3}\left\{\mathrm{Re}^3 \cdot Ro^4\left(3h_r\left(5 + 2K + 6h(1+K) + 2(1+K)\, r \cdot h_{rr}\right) + \left(5 + 2K + 6h(1+K)\right)\, r \cdot h_{rr}\right)\right\}$$

$$C_3 = \frac{1}{240(1+K)^3}\left\{\mathrm{Re}^3 \cdot Ro^4\left((9K-1) r \cdot h_r^2 + 3h_r\left(h(3+5K) + (K-1)\, r^2 \cdot h_{rr}\right) + h \cdot r\left((9K-1)h_{rr} + (K-1)\right)\, r \cdot h_{rrr}\right)\right\}$$

$$C_4 = -\frac{1}{96(1+K)^2 \cdot r^2 \cdot \Delta}\Big(\mathrm{Re} \cdot Ro^2\Big(\left(24r^2 \cdot \mathrm{Re}^2 \cdot Ro^2 - 3K^2(1+K)\,\Delta\right)\, h_r + r\Big(\left(-16 \cdot \mathrm{Re}^2 \cdot Ro^2 + 3K^2(1+K)\,\Delta\right)\, h_{rr} + r\Big(\left(-6r^2 \cdot \mathrm{Re}^2 \cdot Ro^2 + 6K^2(1+K)\,\Delta\right)\, h_{rrr} + K^2(1+K)\, r \cdot \Delta \cdot h_{rrrr}\Big)\Big)\Big)\Big)$$

https://doi.org/10.1017/jmech.2011.11 Published online by Cambridge University Press

$$C_5=\frac{1}{24K(1+K)^2\cdot r^2\cdot\Delta}\Big\{\mathrm{Re}\Big(9r^3\cdot\mathrm{Re}^2\cdot Ro^4\cdot h_r{}^2+\Big(-6h\cdot r^3\cdot\mathrm{Re}^2\cdot Ro^4+2Fr\cdot K(1+K)r\cdot\Delta\Big)\ h_{rr}$$
$$+h_r\left(18h\cdot r^2\cdot\mathrm{Re}^2\cdot Ro^4-2Fr\cdot K(1+K)\ \Delta+3r^4\cdot\mathrm{Re}^2\cdot Ro^4\cdot h_{rr}\right)$$
$$-3h\cdot r^4\cdot\mathrm{Re}^2\cdot Ro^4\cdot h_{rrr}+2K^2\cdot S\cdot\alpha^2\cdot\Delta\cdot h_{rrr}-2K\cdot r\cdot S\cdot\alpha^2\cdot\Delta\cdot h_{rrrr}$$
$$-2K^2\cdot r\cdot S\cdot\alpha^2\cdot\Delta\cdot h_{rrrr}-2K(1+K)r^2\cdot S\cdot\alpha^2\cdot\Delta\cdot h_{rrrrr}\Big)\Big\}$$

$$C_6=\frac{1}{48K(1+K)^3\cdot r^2\cdot\Delta}\Big(\mathrm{Re}\Big(6K\cdot r^2\cdot Ro^2\left(3K(1+K)^2-4h^2(K-1)r^2\cdot\mathrm{Re}^2\cdot Ro^2\right)\ \Delta\cdot h_r{}^3+6h(K+K^2)^2\cdot r^3\cdot Ro^2\cdot\Delta\cdot h_{rr}{}^2$$
$$+2K\cdot r\cdot\Delta\cdot h_r{}^2\left(-6Fr(1+K)^2+9h\cdot K(1+K)^2\cdot Ro^2+2h^3\left(9-22K+10h(1+K)\right)\ r^2\cdot\mathrm{Re}^2\cdot Ro^4+3K(1+K)^2r^2\cdot Ro^2\cdot h_{rr}\right)$$
$$-12Fr\cdot h\cdot K^3\cdot r^2\cdot\Delta\cdot h_{rrr}+18h^2\cdot K^4\cdot r^2\cdot Ro^2\cdot\Delta\cdot h_{rrr}+2h^4\cdot K\cdot r^4\cdot\mathrm{Re}^2\cdot Ro^2\cdot\Delta\cdot h_{rrr}-2h^4\cdot K^2\cdot r^4\cdot\mathrm{Re}^2\cdot Ro^4\cdot\Delta\cdot h_{rrr}$$
$$-12h\cdot K\cdot S\cdot\alpha^2\cdot\Delta\cdot h_{rrr}-24h\cdot K^2\cdot S\cdot\alpha^2\cdot\Delta\cdot h_{rrr}-12h\cdot K^3\cdot S\cdot\alpha^2\cdot\Delta\cdot h_{rrr}$$
$$+K\cdot r\cdot\Delta\cdot h_{rr}\left(h\left(-12Fr(1+K)^2+9h\cdot K(1+K)^2Ro^2+h^3\left(9-22K+8h(1+K)\right)r^2\cdot\mathrm{Re}^2\cdot Ro^4\right)\right.$$
$$\left.+12(1+K)^2\cdot r\cdot S\cdot\alpha^2\cdot h_{rrr}\right)+3h^2\cdot K^2\cdot r^3\cdot Ro^2\cdot\Delta\cdot h_{rrrr}+6h^2\cdot K^3\cdot r^3\cdot Ro^2\cdot\Delta\cdot h_{rrrr}+3h^2\cdot K^4\cdot r^3\cdot Ro^2\cdot\Delta\cdot h_{rrrr}$$
$$+12h\cdot K\cdot r\cdot S\cdot\alpha^2\cdot\Delta\cdot h_{rrrr}+24h\cdot K^2\cdot r\cdot S\cdot\alpha^2\cdot\Delta\cdot h_{rrrr}+12h\cdot K^3\cdot r\cdot S\cdot\alpha^2\cdot\Delta\cdot h_{rrrr}$$
$$+3K\cdot\Delta\cdot h_r\left(h\left(4Fr(1+K)^2-3h\cdot K(1+K)^2Ro^2+h^3\left(1-14K+8h(1+K)\right)r^2\cdot\mathrm{Re}^2\cdot Ro^4\right)\right.$$
$$\left.-4r^2\left(3Fr(1+K)^2-6h\cdot K(1+K)^2Ro^2+2h^3(K-1)r^2\cdot\mathrm{Re}^2\cdot Ro^4\right)h_{rr}\right.$$
$$\left.+4(1+K)^2r\left((h\cdot K\cdot r^2\cdot Ro^2+S\cdot\alpha^2)h_{rrr}+2r\cdot S\cdot\alpha^2\cdot h_{rrrr}\right)\right)+12h\cdot K\cdot r^2\cdot S\cdot\alpha^2\cdot\Delta\cdot h_{rrrrr}$$
$$\left.+24h\cdot K^2\cdot r^2\cdot S\cdot\alpha^2\cdot\Delta\cdot h_{rrrrr}+12h\cdot K^3\cdot r^2\cdot S\cdot\alpha^2\cdot\Delta\cdot h_{rrrrr}-18K^2\cdot r^2\cdot\mathrm{Re}\cdot Ro^2\cdot h_{tr}-6(1+K)^2r^3\cdot\mathrm{Re}\cdot Ro^2\cdot h_{trr}\right)\Big)$$
$$C_7=C_8=0$$

APPENDIX B

The generalized nonlinear kinematic equation

$$h_t+A(h)\ h_r+B(h)\ h_{rr}+C(h)\ h_{rrr}+D(h)\ h_{rrrr}+E(h)\ h_r^2+F(h)\ h_r\ h_{rrr}=0$$

where

$$A(h)=\frac{h^2\cdot\mathrm{Re}\left(15h\cdot(1+K)^2\cdot(-16Fr+15h\cdot K\cdot Ro^2)\cdot\alpha+2r^2\cdot Ro^2\left(360(1+K)^2+h^4\left(73-303K+146h\cdot(1+K)\right)\mathrm{Re}^2\cdot Ro^2\cdot\alpha\right)\right)}{720(1+K)^3r}$$

$$B(h)=-\frac{h^3\cdot\mathrm{Re}\left(80Fr\cdot(1+K)^2\cdot125h\cdot K(1+K)^2\cdot Ro^2\right)+18h^3\cdot(-1+K)\cdot r^2\cdot\mathrm{Re}^2\cdot Ro^4)\cdot\alpha}{240(1+K)^3}$$

$$C(h)=\frac{h^3\cdot\mathrm{Re}\cdot\alpha\left(5(4+h)\cdot K\cdot r^2\cdot Ro^2+16S\cdot\alpha^2\right)}{48(1+K)\cdot r}$$

$$D(h)=\frac{h^3\cdot\mathrm{Re}\cdot S\cdot\alpha^3}{3(1+K)}$$

$$E(h)=-\frac{h^2\cdot\mathrm{Re}\left(20Fr(1+K)^2+h\cdot Ro^2(-25K-50K^2-25K^3-9h^2\cdot r^2\cdot\mathrm{Re}^2\cdot Ro^2+9h^2\cdot K\cdot r^2\cdot\mathrm{Re}^2\cdot Ro^2)\right)\cdot\alpha}{120(1+K)^3}$$

$$F(h)=-\frac{h^2\cdot\mathrm{Re}\cdot S\cdot\alpha^3}{(1+K)}$$

https://doi.org/10.1017/jmech.2011.11 Published online by Cambridge University Press

REFERENCES

1. Yang, Y. K. and Chang, T. C., "Experimental Analysis and Optimization of a Photo Resist Coating Process for Photolithography in Wafer Fabrication," *Microelectronics Journal,* **37**, pp. 746–751 (2006).
2. Kuo, Y. K. and Chao, C. G., "Control Ability of Spin Coating Planarization of Resist Film and Optimal of Developers," *Microelectronics Journal,* **37**, pp. 759–764 (2006).
3. Emslie, A. G., Bonner, F. T. and Peck, L. G., "Flow of a Viscous Liquid on a Rotating Disk," *Journal of Applied Physics,* **29**, pp. 858–862 (1958).
4. Higgins, B. G., "Film Flow on a Rotating Disk," *Physics of Fluids,* **29**, pp. 3522–3529 (1986).
5. Kitamura, A., Hasegawa, E. and Yoshizawa, M., "Asymptotic Analysis of the Formation of Thin Liquid Film in Spin Coating," *Fluid Dynamics Research*, **30**, pp. 107–125 (2002).
6. Lin, C. C., *The Theory of Hydrodynamic Stability*, Cambridge University Press. (1955).
7. Chandrasekhar, S. *Hydrodynamic and Hydromagnetic Stability*, Oxford University Press. (1961).
8. Kapitza, P. L., "Wave Flow of Thin Viscous Liquid Films," *Zhurnal Èksperimentalnoi I Teoreticheskoi Fiziki,* **18**, pp. 3–28 (1949).
9. Benney, D. J., "Long Waves on Liquid Film," *Journal of Mathematical Physics,* **45**, pp. 150–155 (1966).
10. Landau, L. D., "On the Problem of Turbulence," *Comptes Rendus (Doklady) of Academy of sciences,* **44**, pp. 311–314 (1944).
11. Yih, C. S., "Stability of Liquid Flow Down an Inclined Plane," *Physics Fluids,* **6**, pp. 321–334 (1963).
12. Stuart, J. T. "On the Role of Reynolds Stresses in Stability Theory," *Journal of the Aeronautical Sciences,* **23**, pp. 86–88 (1956).
13. Pumir, A., Manneville, P. and Pomeau, Y., "On Solitary Waves Running Down on Inclined Plane," *Journal of Fluid Mechanics,* **135**, pp. 27–50 (1983).
14. Ruyer-Quil, C. and Manneville, P., "Modeling Film Flows Down an Inclined Planes," *European Physical Journal,* **B 6**, pp. 277–292 (1998).
15. Ruyer-Quil, C. and Manneville, P., "Improved Modeling of Flows Down Inclined Planes," *European Physical Journal,* **B 15**, pp. 357–369 (2000).
16. Ruyer-Quil, C. and Manneville, P., "Further Accuracy and Convergence Results on the Modeling of Flows Down Inclined Planes by Weighted Residual Approximations," *Physics of Fluids,* **14**, pp. 170–183 (2002).
17. Amaouche, M., Mehidi, N. and Amatousse, N., "An Accurate Modeling of Thin Film Flows Down an Inclined for Inertia Dominated Regimes," *European Journal of Mechanics B/Fluids,* **24**, pp. 49–70 (2005).
18. Samanta, A., "Stability of Liquid Film Down a Vertical Non-Uniformly Heated Wall," *Physica D: Nonlinear Phenomena*, **237**, pp. 2587–2598 (2008).
19. Eringen, A. C., "Theory of Micropolar Fluids," *Journal of Mathematics Mechanics,* **16**, pp. 1–18 (1967).
20. Hung, C. I., Tsai, J. S. and Chen, C. K., "Nonlinear Stability of the Thin Micropolar Liquid Film Flowing Down on a Vertical Plate," *Journal of Fluids Engineering,* ASME, **118**, pp. 498–505 (1996).
21. Dupuy, D. G., Panasenko, P. and Stavre, P., "Asymptotic Analysis for Micropolar Fluids," *Comptes Rendus Mecanique,* **332**, pp. 31–36 (2004).
22. Chen, C. I., "Non-Linear Stability Characterization of the Thin Micropolar Liquid Film Flowing Down the Inner Surface of a Rotating Vertical Cylinder," *Communications in Nonlinear Science and Numerical Simulation*, **12**, pp. 760–775 (2007).
23. Ahmadi, G., "Self-Similar Solution of Incompressible Micropolar Boundary Layer Flow Over a Semi-Infinite Plate," *International Journal of Engineering Science,* **14**, pp. 639–646 (1976).
24. Jena, S. K. and Mathur, M. N., "Mixed Convenction Flow of a Micropolar Fluid from an Isothermal Vertical Plate," *Mathematics Applied,* **10**, pp. 291–304 (1984).
25. Ginzburg, V. L. and Landau, L. D., "Theory of Superconductivity," *Journal of Experimental and Theoretical Physics,* **120**, pp. 1064–1082 (1950).
26. Cheng, P-J. and Lai, H-Y., "Nonlinear Stability Analysis of Thin Film Flow from a Liquid Jet Impinging on a Circular Concentric Disk," *Journal of Mechanics*, **22**, pp. 115–124 (2006).

(Manuscript received December 21, 2009,
accepted for publication May 26, 2010.)

https://doi.org/10.1017/jmech.2011.11 Published online by Cambridge University Press